

SCIENCE OF TSUNAMI HAZARDS

Journal of Tsunami Society International

Volume 30

Number 4

2011

OBSERVATION OF TSUNAMI RADIATION AT TOHOKU BY REMOTE SENSING

Frank C. Lin^{1*}, Weiwei Zhu^{1**}, Kingkarn Sookhanaphibarn²

¹Dept. of Mathematics and Computer Science
University of Maryland Eastern Shore
Princess Anne, MD. 21853, U.S.A.

²Intelligent Computer Entertainment Laboratory
Dept. of Human and Computer Intelligence
Ritsumeikan University
1-1-1 Noji Higashi, Kusatsu, Shiga, 525-8577, Japan

ABSTRACT

We present *prima facie* evidence that upon the onset of the Tohoku tsunami of Mar. 11, 2011 infrared radiation was emitted by the tsunami and was detected by the Japanese satellite MTSAT-IR1, in agreement with our earlier findings for the Great Sumatra Tsunami of 2004. Implications for a worldwide Tsunami Early Warning System are discussed.

Keywords: *Tsunami, Tsunami Radiation, Tsunami Signal, Tsunami Early Warning System, Tohoku*

*Corresponding author. Email: linbfrank@gmail.com. Tel/Fax: +662 612 4705. **wzhu@umes.edu. #kingkarn@ice.ci.ritsumei.ac.jp.

1. INTRODUCTION

In previous communications (Na Nakornphanom et al. 2007; Lin et al. 2010; Lin and Sookahanaphibarn 2011) we have provided clear evidence that at the *birth* of a tsunami, as the cold water is lifted to the surface of the ocean, the tsunami *emits an infrared radiation of 11 ± 0.5 microns*, which being in the thermal range can be detected by satellites. We have shown that this radiation is captured by the infrared sensors of the Chinese Meteorological Satellite FY-2C, which is geostationary at Lon 105°E and Lat 0°N, as well as by the NOAA V5 Pathfinder satellite. We have investigated seven earthquake locations in the Indian Ocean on Dec. 26, 2004 including the Main Event at Banda Aceh. We found that of these seven earthquakes there were five that emitted the telltale tsunami signal whereas in two cases no radiation was detected, indicating that these respective earthquakes, though of comparable magnitude, did not spawn a tsunami. This *Sachverhalt* has obviously important implications for the reliability of tsunami early warning systems, which we shall discuss subsequently. Noise such as cloud or heat emanating from landmass has been accounted for.

In this paper we shall apply the same methodology to the Tohoku tsunami of Mar. 11, 2011. The tsunami radiation has been, as expected, captured by the MTSAT-IR1 satellite of the Japan Meteorological Society. The present work confirms the validity of our previous approach in a different geophysical context and for several new events. Some speculative suggestions for possible predictions of future events based on the pattern of foreshocks are considered.

The Tohoku events that we investigate in this paper are listed in the Table below, together with their attributes:

Table 1: Tohoku Earthquake Events and Attributes.

Event	Me	Time UTC	Latitude in degrees	Latitude in pixels	Longitude in degrees	Longitude in pixels	Signal at Epicenter, S in pixels	M _t Eq.1
Main-shock	9.0	05:46	38.297N	38	142.372E	142	255	7.99
Foreshock	7.2	02:45	38.424N	145	142.636E	186	197	7.62
Aftershock-1	7.1	14:32	38.253N	145	141.640E	181	161	7.33
Aftershock-2	6.6	08:16	37.007N	261	140:477E	207	none	

2. THE MAIN EVENT

On Friday, March 11, 2011 at 05:46:24 UTC (02:46:24 p.m. local time) at the location 38.297°N and 142.372°E at the depth of 30 km and at a distance of 129 km East of Sendai, Honshu, Japan an earthquake of magnitude 9.0 occurred. According to the Jet Propulsion Laboratory of Caltech (Caltech 2011), the coast of northeast Japan moved eastward up to 4 meters and the coastline generally subsided up to 1.1 meters. This is due to the fault at the subduction zone between the Pacific and the North American plates. The Pacific plate moved westwards descending beneath Japan. The slip was

approximately 300 km long and 150 km wide. At least 15,703 people were killed and at least 332,395 buildings destroyed or damaged by the earthquake and tsunami along the entire east coast of Honshu. The tsunami runup height was 37.88 m at Miyako. The economic loss in Japan is estimated to be more than 300 billion U.S. dollars. In addition, several reactors were damaged at Fukushima and leaked radiation, posing a health hazard. Both life and property damages were sustained in other parts of the world.

Evidently, the Early Warning System in Japan was inadequate to cope with a disaster of this magnitude. Our proposal of detecting the *birth* of tsunamis by remote sensing could possibly enhance the warning system and save life and property in future.

The following cropped satellite image was recorded by the MTSAT-IT1 on 2011-03-11 at 06:30 UTC at latitude 38.322°N. According to our previous work, the tsunami radiation should be visible in the infrared domain, provided that the cool water from the bottom of the ocean has reached the ocean surface (Lin et al. 2010).

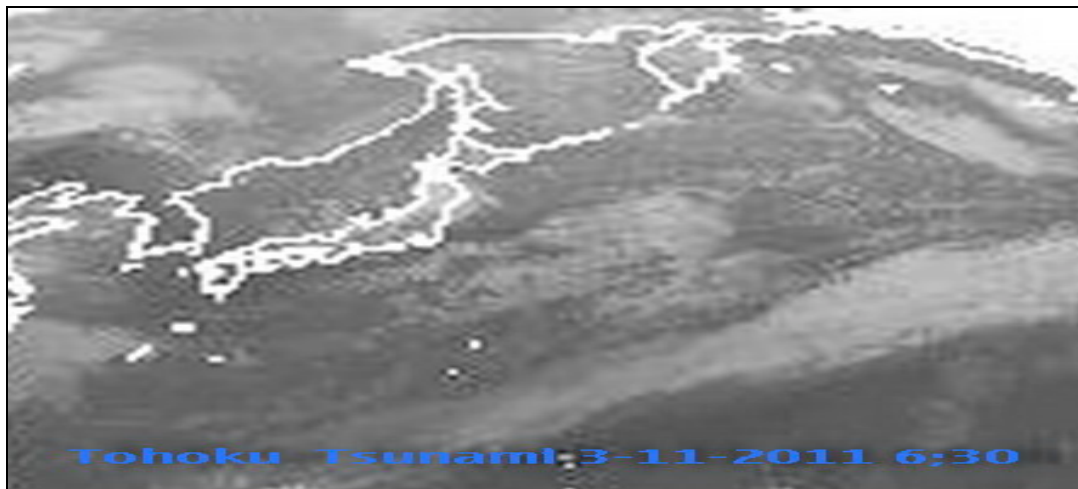


Fig.1: Satellite Image of the Main Event for the Tohoku Tsunami of 2011-03-11

In Fig.2 we show the Signal Diagram for the aforementioned latitude and we discern indeed a spike at the location of the undersea earthquake corresponding to the thermal emission detected by the satellite. This confirms the validity of our procedure previously applied to the Great Sumatra Tsunami in the Indian Ocean, albeit for a high latitude event, where the water temperature is significantly lower. An arrow points to the tsunami signal.

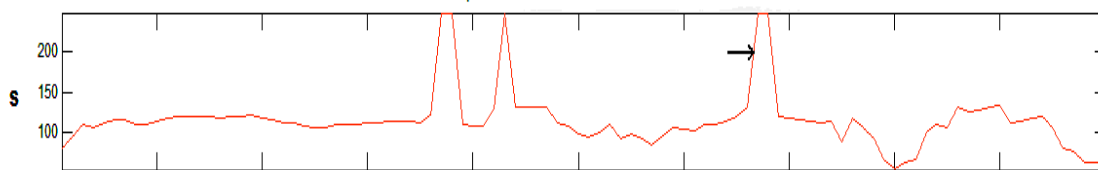


Fig.2: Signal Diagram of Tohoku Main Event of 2011-3-11

The Wavelet Diagram for this event is shown in Fig.3. Again, an arrow points to the tsunami signal. As before, the Haar mother-wavelet is selected.

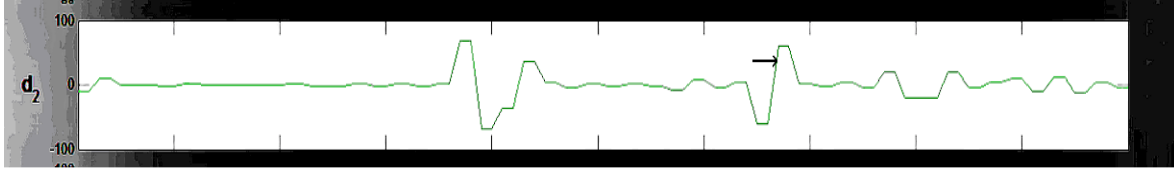


Fig.3: Wavelet Diagram of Tohoku Main Event of 2011-3-11

Regarding the horizontal scale, all Signal Diagrams encompass 500 pixels between notches and all Wavelet Diagrams span 200 pixels between notches unless otherwise labeled. For the vertical scale, the range of Signal Diagrams is from 0 to 250, and the range for Wavelet Diagrams is from -100 to +100 unless otherwise labeled

3. FORESHOCKS AND AFTERSHOCKS

The Main Event was preceded by numerous foreshocks and followed by hundreds of aftershocks. On March 9, 2011, at 02:45 UTC a foreshock of magnitude 7.2 occurred at latitude 38.424°N and longitude 142.836°E at the depth of 32 km. We examined the satellite image for 03:32 UTC at this latitude. Fig. 4 shows the corresponding Signal Diagram.

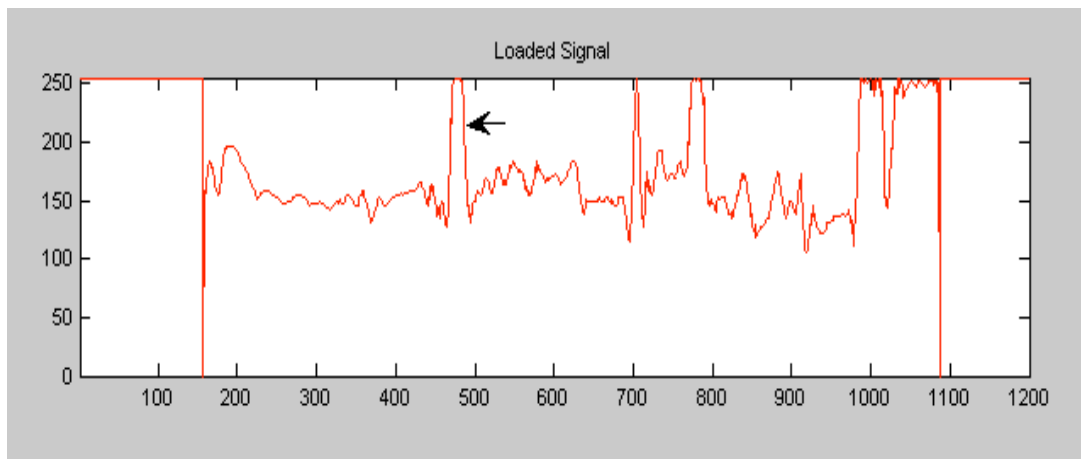


Fig. 4: Signal Diagram of Tohoku Foreshock of 2011-3-9

It is seen that at the location of the undersea earthquake, a distinct tsunami signal is found indicating that the cool ocean water from the bottom has reached the surface and thus was detected by the satellite. An arrow again points to the tsunami signal. This is the first time that this

phenomenon has been associated with a foreshock. Since 1973, there were 9 earthquakes on the Japan trench with $M_e \geq 7$. This suggests that the Main Event could possibly have been predicted if all significant foreshocks were taken into account, by e.g. using a Neural Network (Lin and Mohamed 1999; Lin et al. 2002). The corresponding Wavelet Diagram, where an arrow points to the Tsunami Signal, is shown in Fig 5 below:

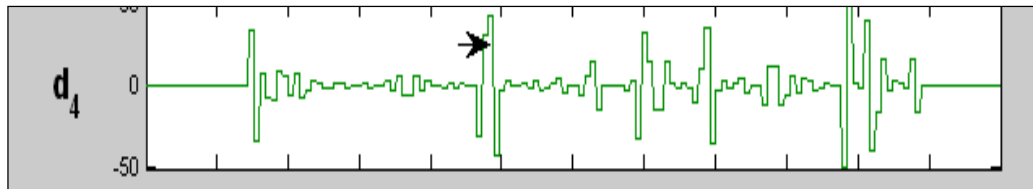


Fig.5: Wavelet Diagram of Tohoku Foreshock of 2011-3-9

There were 4 major aftershocks after the Main Event: On Mar. 11 at 06:15 UTC a magnitude 7.9 aftershock occurred at 36.27°N and 141.14°E; at 06:25 UTC on the same day, a magnitude 7.7 aftershock occurred at 38.05°N and 144.59°E; on Apr. 7, 2011 at 14:32 UTC a magnitude 7.1 aftershock occurred at 38.253°N and 141.640°E; and on Apr. 11, 2011 at 08:16 UTC a magnitude 6.6 aftershock occurred at 37.007 °N and 140.477°E. We shall call the last two Aftershock-1 and Aftershock-2. The satellite images were recorded at 15:33 UTC and 08:32 UTC respectively.

We obtained for Aftershock-1 the following Signal and Wavelet diagrams.

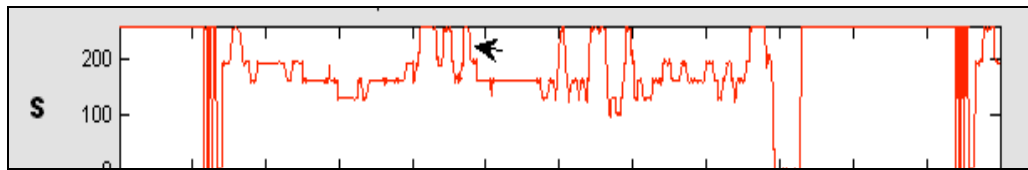


Fig.6: Signal Diagram of Tohoku Aftershock-1

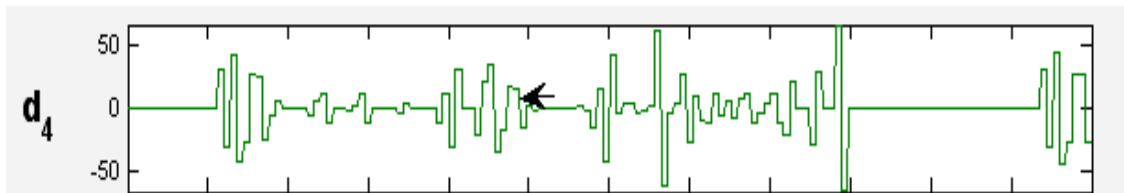


Fig.7: Wavelet Diagram for Tohoku Aftershock-1

An arrow points to the tsunami signal for Aftershock-1. Although the cold water has reached the ocean surface, it did not cause widespread damage. The propagation of tsunamis in infrared space is the subject of future research.

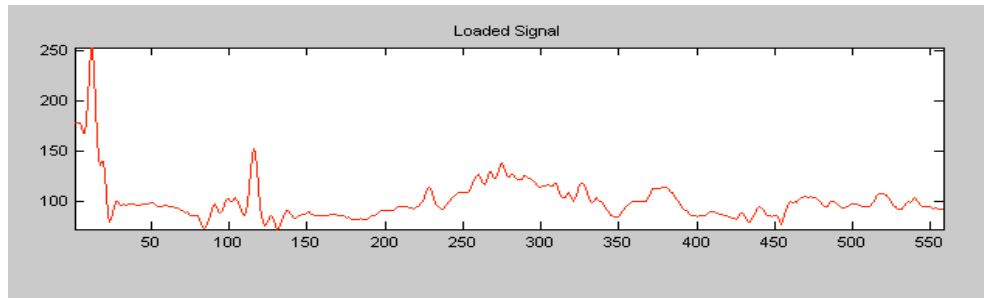


Fig.8: Signal Diagram for Tohoku Aftershock-2

Aftershock-2 is an interesting case in that no tsunami signal is discernible at longitude 140.477°E or pixel value 207 (see Fig. 8). This is probably due to the fact that the satellite image was taken only sixteen minutes after the earthquake was detected. This may not have provided adequate time for sufficient quantity of cold water to reach the ocean surface in order to trigger the tsunami signal. Alternately, and perhaps more likely, the cold water may not have breached the ocean surface at all, as some cases in the Indian Ocean that we have investigated (Lin et al. 2010). The thermodynamic and hydrodynamic mechanism by which the cold water is lifted to the ocean surface has yet to be elucidated.

IV. Tsunami Magnitude

We define the Tsunami Magnitude *in infrared space*, in analogy to the definition of Iida et al. (1967) in visible space, as follows:

$$M_t = \log_2 S \quad (1)$$

where

M_t = Tsunami Magnitude,

S = Tsunami Signal (Pixel brightness at the epicenter. See Table 1 for numerical values obtained directly from the satellite images).

Similarly, the Tsunami Intensity can be defined as:

$$I_t = \log_2 (\sqrt{2} * S) \quad (2)$$

In visible space (Rastogi and Jaiswal 2006) S is the estimated maximum run up height of the wave. This measure has been suggested based on the effect and damage caused by the tsunami. The velocity of a tsunami in the open ocean is given by

$$V = (dg)^{1/2} \quad (3)$$

where d is the ocean depth and g the acceleration of gravity.

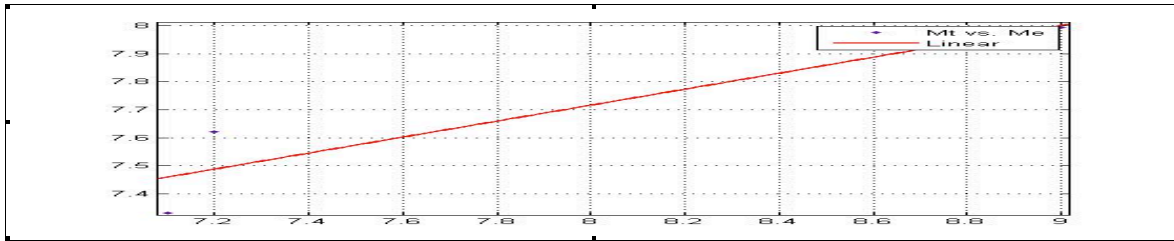


Fig.9: Earthquake Magnitude versus Tsunami Magnitude

Using the data from Table 1, a linear interpolation of Tsunami Magnitude versus Earthquake Magnitude is given in Fig. 9. We have shown in (Lin and Sookhanaphibarn 2011) that all tsunami representations must be linear. In general, the tsunami magnitudes are 10% less than those of the Indian Ocean (Lin et al. 2010). This is probably due to the greater temperature gradient of the latter.

5. EARLY WARNING BY REMOTE SENSING (REMOTE)

At the onset of a tsunami event, the cold water is lifted up to the surface. The tsunami burst is therefore characterized by a temperature gradient. Meteorological satellites such as the Chinese FY-2C, recording between the wavelengths 10.5 and 12.5 μm , is able to detect this temperature gradient.

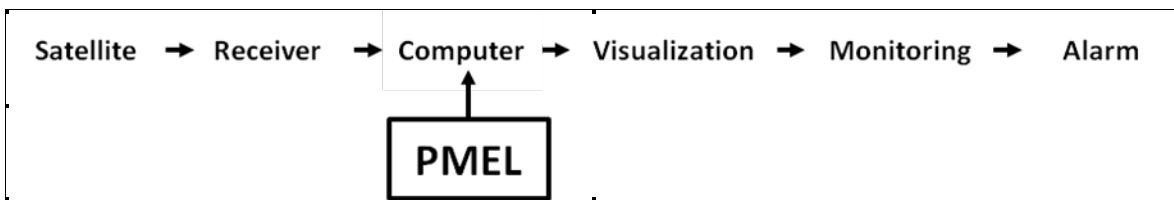


Fig.10: Early warning system

Our method consists of using an antenna and receiver to capture the tsunami radiation in infrared domain. A PC producing visualizations that we have shown in the figures in this paper processes this signal. At the same time undersea earthquake activities are collected in real time from watchdogs such as PMEL (Fig. 10). The visualization will then confirm or refute the birth of a tsunami associated with this earthquake, such that a warning can be instantly and automatically issued.

6. COMPARISON WITH DART

Present methods such as “The Deep-ocean Assessment and Reporting of Tsunami” (DART) to detect tsunamis measure aquatic pressure changes due to submarine earthquakes. The DART system functions as follows: Pressure sensors are placed at the ocean bottom near the earthquake zone. An acoustic modem transducer encodes the data into sound waves. A communications buoy processes the information and sends it by radio waves to a weather satellite (GOES). Computers at ground station calculate tsunami’s starting point, speed and arrival times.

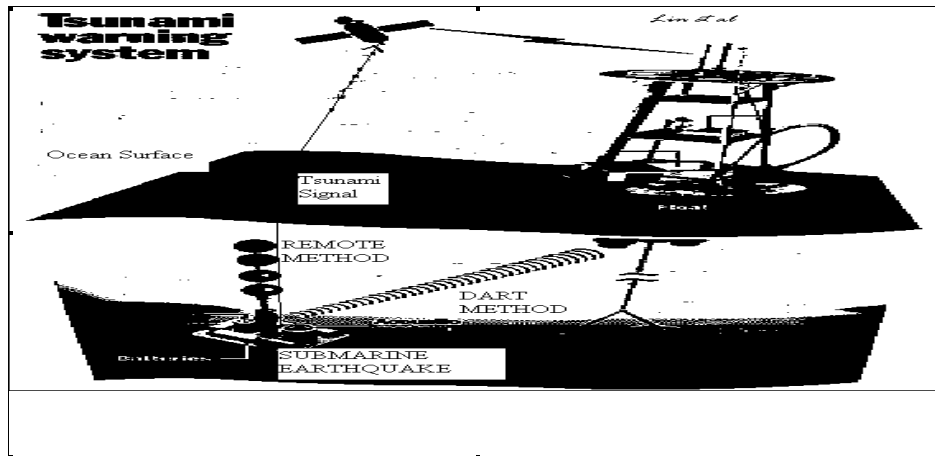


Fig.11: DART vs. REMOTE

The above Figure (Fig.11) shows the *modus operandi* of the two systems. We shall consider the following discussion points in comparing the DART and REMOTE methods: 1) Time Delay, 2) Cost, 3) Reliability and 4) Availability.

1) Time Delay: For the DART System, the earthquake is registered by an underwater pressure gauge, which forwards this information acoustically to a buoy at the surface of the ocean. Since the signal travels at the speed of sound over hundreds of kilometers, a time lapse is incurred. In the Mentawai tsunami of 2010, for instance, it took one hour for the information to reach the first buoy and another hour to reach the second buoy. *This time lapse is critical for the effectiveness of Early Warning.* An hour also lapsed between the Tohoku Main Event and when the tsunami reached the Fukushima nuclear plant.

In our REMOTE system, as soon as the cold water reaches the surface of the ocean, an infrared radiation (called the Tsunami Signal) is emitted which travels to the satellite at the speed of light, i.e. instantaneously. No time delay is thereby incurred.

2) Cost: An individual buoy costs over one million dollars to put in place. Its maintenance is generally beyond the financial capability of poorer nations. Many buoys are needed to adequately protect an extended coastline. In the REMOTE system, just one setup is sufficient to protect a country, provided that it has access to a weather satellite. The initial cost is less than a hundreds of that of a buoy and the maintenance cost is minimal.

3) Reliability: The pressure changes as measured by DART may not trigger a tsunami, and consequently the present method yields high rates of false positive alarms. According to reports from NOAA and others (Gonzalez 1999), approximately 75% of all warnings issued since 1948 have been false. The REMOTE method will broadcast a warning if and only if the cold water has reached the surface of the ocean and is thus more reliable.

4) Availability: At present, some 39 buoys have been implemented, mostly along the Pacific Rim. Large segments of the earth, such as the Indian Ocean, the Mediterranean Ocean and South America are not yet safeguarded.

7. CONCLUSION

We have made the remarkable finding that as the cold water from the bottom of the ocean is lifted up to the ocean surface by a submarine earthquake it emits an infrared radiation centered around 11 microns which can be detected by a satellite. We used this tool to investigate tsunami events of Dec. 26, 2004 in the Indian Ocean (Lin et al. 2010) and of Mar. 11, 2011 in the Tohoku region. It is found that each event will either send out this tsunami signal signifying the birth of a tsunami, or no signal is sent in which case no Tsunami Warning should be issued. There is therefore no false positives or false negatives. In comparison to DART, it is ascertained that this system, called REMOTE, has essentially no time delay, is orders of magnitude less expensive, unambiguous and can be easily made available to the world thereby substantially improving and augmenting the saving of life and property.

REFERENCES

- Caltech (2011): <ftp://sideshow.jpl.nasa.gov/pub/usrs/ARIA>. See also <http://earthquake.usgs.gov/earthquakes/eqinthenews/2011/usc0001xgp/> (2011).
- Elborn, S. and F.C.Lin (1992), Analysis & Prediction of Earthquakes for Southern California Using A Neural Network. *Geologia Applicata e Idrogeologia* Vol.xxvii, pp.111-121, Bari, Italy.
- Gonzalez, F. (1999), TSUNAMI!, *Scientific American*, 280, 56-65
- Iida, K, Cox D. and Pararas-Carayannis G. (1967), Preliminary Catalog of Tsunamis Occurring in the Pacific Ocean. Hawaii Institute of Geophysics, Honolulu, HI, August (Rept. HIG- 67-10)
- Lin, F.C. and I. Panikkar (1995), Study of Seismic Activity in Central Asia Applying A Parallel Distributed Paradigm. Proceedings of the 1995 International Geoscience & Remote Sensing Symposium, Firenze, Italy, July 10-14
- Lin, F.C. Lin and I.E. Mohamed (1999), Predicting Seismic Aftershocks Using a Neural Network. Proceedings of the International Geoscience & Remote Sensing Symposium (IGARSS '99), Hamburg, Germany
- Lin, F.C., N. Elhassan, A. Hassan and A. Yousif (2002), Forecast of Seismic Aftershocks using a Neural Network. Proceedings of the 9th International Conference on Neural Information Processing, Singapore

Lin, F.C., K. Na Nakornphanom, K. Sookhanaphibarn, and C. Lursinsap (2010), A New Paradigm for Detecting Tsunamis by Remote Sensing. *Int. Journal of Geoinformatics*, 6(1), 19-30.

Lin, F.C. and K. Sookhanaphibarn (2011), Representation of Tsunamis in Generalized Hyperspace. *Proceedings of the IEEE International Geoscience and Remote Sensing Symposium (IGARSS'11)*, Sendai/Vancouver, July 21, 2011. pp. 4355-4358

Na Nakornphanom, K., Frank C. Lin and C. Lursinsap (2007), Tsunami Detection and Early Warning by TIR Remote Sensing. *Proceedings of The Third Shanghai International Symposium on Nonlinear Sciences and Applications*, June 6-10

Rastogi, B.K. and Jaiswal, R.K. (2006), A Catalog of Tsunamis in the Indian Ocean, *Science of Tsunami Hazards*, 25(3), p. 128.